

Observation of NH₂ species on tilted InN (011̄1) facets

A. R. Acharya, M. Buegler, R. Atalay, N. Dietz, and B. D. Thoms^{a)}
Department of Physics and Astronomy, Georgia State University, Atlanta, Georgia 30303

J. S. Tweedie and R. Collazo
Department of Materials Science and Engineering, North Carolina State University, Raleigh, North Carolina 27695

(Received 14 January 2011; accepted 10 May 2011; published online 15 June 2011)

The structural properties and surface bonding configuration of InN layers grown by high-pressure chemical vapor deposition have been characterized using Raman spectroscopy, x-ray diffraction (XRD), and high resolution electron energy loss spectroscopy. The appearance of the A₁(TO) mode at 447 cm⁻¹ in unpolarized $z(\cdot)\bar{z}$ Raman spectrum indicates distortions in the crystal lattice due to the growth of tilted plane crystallites. A Bragg reflex in the x-ray diffraction spectrum at $2\Theta \approx 33^\circ$ has been assigned to tilted InN facets in the polycrystalline InN layer. The high resolution electron energy loss spectrum for this InN layer features vibration modes assigned to NH₂ species indicating a surface orientation consistent with the crystalline properties observed in Raman spectroscopy and XRD. The appearance of tilted planes is suggested to be due to the effects of high V–III ratio and lattice mismatch on the growth mechanism. © 2011 American Vacuum Society. [DOI: 10.1116/1.3596619]

I. INTRODUCTION

Since the first attempt to synthesize InN by Juza and Hahn in 1938,¹ the interest in studying and understanding the revised physical properties of InN has been growing significantly due to its highly attractive optoelectronic properties. During the last 10 years, it has been shown that InN is a narrow bandgap semiconductor (~ 0.7 eV) with potential for a wide range of applications, including chemical and biological sensors,² high electron mobility transistors,³ multijunction tandem solar cells,⁴ thermoelectric devices,⁵ and terahertz radiation devices.⁶ InN is the binary corner for ternary (InGa_xN and InAl_{1-x}N) and quaternary (InGa_xAl_{1-x}N) group III-nitride alloys, which are presently explored for frequency agile detectors and emitters operating from ultraviolet (UV) to near infrared (IR) region. For instance, along with GaN, ternary InGa_xN alloys are integrated in a variety of heterostructure-based optoelectronic devices, such as light emitting diodes (LED),^{7,8} laser diodes,⁹ or in unique detectors that cover the wavelength regime from UV down to the far IR.¹⁰ InN is predicted to have the lowest effective electron mass of all III-nitride semiconductors,¹¹ enabling device elements with high mobility and high saturation drift velocity.

The growth of high crystalline quality InN and indium-rich group III-nitride alloys remains a challenge—mainly due to the low dissociation temperature of InN. Thermal dissociation can be avoided by growing at low enough temperatures, about 600°C for low-pressure chemical vapor deposition.¹² The cracking efficiency of ammonia in this temperature regime is extremely low, requiring a large group V–III precursor ratio.¹³ Highly volatile compounds, such as InN and related alloys, can be grown at much higher temperatures if surface stabilization is done at high pressures.^{14,15} In order to stabilize InN growth at elevated temperatures, high-pressure chemical vapor deposition (HPCVD) has been

found to be an effective technique for producing high quality III–N layers.¹³

Growth of III-nitride-based semiconductors in the *c* direction may be preferred because of the cost-effective fabrication of the devices. However, due to the lattice geometry and the induced strain, large piezoelectric fields are present within the heterostructures.¹⁶ In optoelectronic devices, the spontaneous and piezoelectric polarizations affect the internal quantum efficiency of the quantum well structures.¹⁷ Despite the present difficulty in the device fabrication, new approaches have been explored, e.g., growth on tilted or various nonpolar (*a*, *r*, and *m*) planes.^{18,19} It has been shown that layers grown on *a* or *m* plane increase the efficiency of the devices as the polarization effects are minimized. Ahn *et al.*²⁰ reported two orders of magnitude increase in the terahertz emission from *a*-plane compared to *c*-plane InN.

Other properties such as stability are also affected by the surface orientation of InN layers. Naoi *et al.* have reported that the In-polar surface is chemically more stable, whereas the N-polar surface is thermally more stable.²¹ They suggest that differences in chemical reactivity and stability for InN surfaces are related to differences in work function. Similar studies of chemical and thermal stability have not yet been reported for nonpolar or mixed polarity InN planes.

This work uses Raman spectroscopy, x-ray diffraction (XRD), and high resolution electron energy loss spectroscopy (HREELS) to characterize the structure and bonding properties of an HPCVD-grown InN layer exhibiting tilted facets. In addition, the relationship of the growth conditions to the production of tilted facets on the InN surface is discussed.

II. EXPERIMENTAL METHODS

The InN layer analyzed in this work was grown by HPCVD at a growth temperature of 865°C, a reactor pressure of 15 bar, and an ammonia (NH₃) to trimethylindium

^{a)}Electronic mail: bthoms@gsu.edu

(TMI) precursor ratio of 3000. The layer was deposited directly on a sapphire (0001) substrate. In previous work, studies on InN layers grown on GaN buffer layers on a sapphire (0001) leading to *c*-plane orientation of the layers were reported.²² Details of the HPCVD reactor, the growth configuration, and the real-time optical characterization techniques employed have been published elsewhere.^{13,23,24}

For Raman analysis, an excitation source of 532 nm (2.33 eV) was used. The Raman spectrometer consists of a McPherson double subtractive monochromator and a single 2m monochromator system. The Raman measurements were carried out in backscattering geometry. The ω -2 Θ XRD results were obtained utilizing an X'Pert PRO MPD (Philips) 4-circle diffractometer equipped with a monochromatic x-ray (Cu $K\alpha$) source. The sample was aligned prior to the measurements utilizing the substrate's sapphire (0006) Bragg reflex. HREELS, a surface sensitive vibrational technique, was performed in a stainless-steel ultrahigh vacuum (UHV) system with a base pressure of 2×10^{-10} Torr. Bellitto *et al.* have reported the details of the UHV system and sample mount.²⁵ The sample was cleaned with acetone and rinsed with isopropyl alcohol before insertion into the UHV chamber. Inside the UHV chamber, the sample was cleaned by a procedure of bombardment with 1 keV nitrogen ions followed by atomic hydrogen cleaning, which was demonstrated as an effective way to remove surface contaminants by Piper *et al.*²⁶ The removal of surface contaminants (carbon, oxygen) was confirmed by Auger electron spectroscopy (AES). Atomic hydrogen cleaning was performed by back-filling the vacuum chamber with hydrogen to a pressure of 8.4×10^{-7} Torr in the presence of a tungsten filament heated to 1575°C to produce H atoms. The sample was kept at 20 mm from the dosing filament for 5 min (giving an exposure of 250 L of hydrogen, 1 L = 1×10^{-6} Torr s). During this time the sample temperature increased to 60°C due to the heated dosing filament. After 5 min, the sample was heated to 350°C by the bombardment of the electrons from the back of the sample mount for 10 min while H atom exposure continued (giving an additional exposure of 500 L of hydrogen). HREELS experiments were performed in a specular geometry with an incident and scattered angle of 60° from the surface normal, and an incident electron beam energy of 5.6 eV.

III. RESULTS AND DISCUSSION

The Raman spectrum for the InN layer is shown in Fig. 1. The prominent peak at 592.5 cm⁻¹ is assigned to the A₁(LO) vibration mode.²⁷ The broad peak between 405 and 540 cm⁻¹ is deconvoluted to resolve into four significant components using Gaussian line shape analysis as depicted in Fig. 1, with parameters summarized in Table I. The largest peak contribution centered at 489.6 cm⁻¹ has been assigned to E₂(high).^{27,28} The Raman mode centered at 449.6 cm⁻¹ has been assigned to A₁(TO) and the peak centered at 470.4 cm⁻¹ has been assigned to E₁(TO) modes.^{27,29} From the Raman selection rules, however, the mode pairs A₁(LO)–E₂(high) and A₁(TO)–E₁(TO) are forbidden in the same

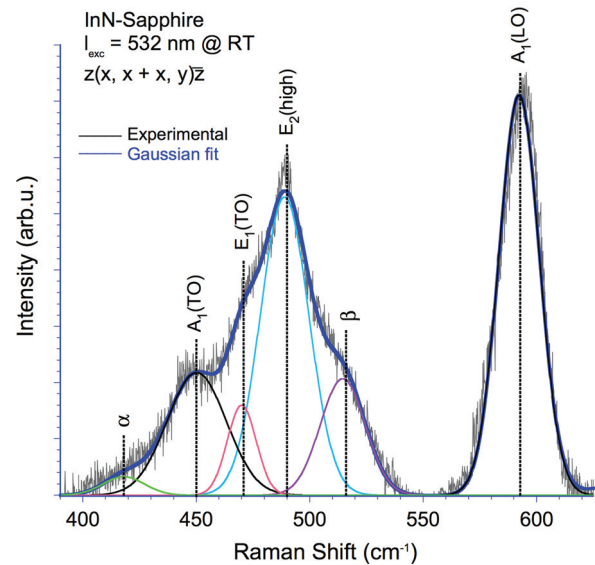


Fig. 1. (Color online) Raman spectrum of an InN layer grown on sapphire with deconvolution of the Raman modes using Gaussian curves.

plane. Thus, the observation of these modes in the Raman spectrum indicates that the layer contains grain facets tilted against the growth direction.

In addition, the weak Raman feature centered at 515.2 cm⁻¹ (denoted by β in Fig. 1) belongs neither to any known InN modes nor to any sapphire substrate related mode of vibration. One possible explanation for this feature might be a second-order Raman effect of the B₁(low) mode. However, Dhara *et al.*³⁰ have interpreted a feature at the same spectral position to disorder assisted longitudinal optical mode.

The x-ray diffraction spectrum for the InN layer recorded in ω -2 Θ geometry is shown in Fig. 2. The XRD spectrum shows a dominant hexagonal InN (0002) Bragg reflex at 31.24° with a FWHM of 536 arcsec, corresponding to a *c*-lattice constant of 5.722 Å. Two additional Bragg reflexes are observed, centered at 32.8° and 33.06°. Shubina *et al.*³¹ assigned the “anomalous” peak in x-ray diffraction pattern at 2 Θ \approx 33° to metallic indium. However, Yu *et al.*³² later suggested that the anomalous 33° peak might be related to the (01 $\bar{1}$ 1) diffraction peak of polycrystalline InN. Our studies found that the peak centered at 32.86° can be assigned to residual metallic indium at the surface, related to the In (101) Bragg reflex (2.723 Å) with a FWHM of 428 arcsec.

TABLE I. Raman spectroscopy results and assignments.

Symmetry mode	Literature value ^a center peak pos. (cm ⁻¹)	Literature value ^b center peak pos. (cm ⁻¹)	Experimental value center peak pos. (cm ⁻¹)
A ₁ (TO)	443	445	449.6
E ₁ (TO)	477	472	470.4
E ₂ ^H	491	488	489.6
β	—	—	515.2
A ₁ (LO)	590	588	592.5

^aReference 27.

^bReference 29.

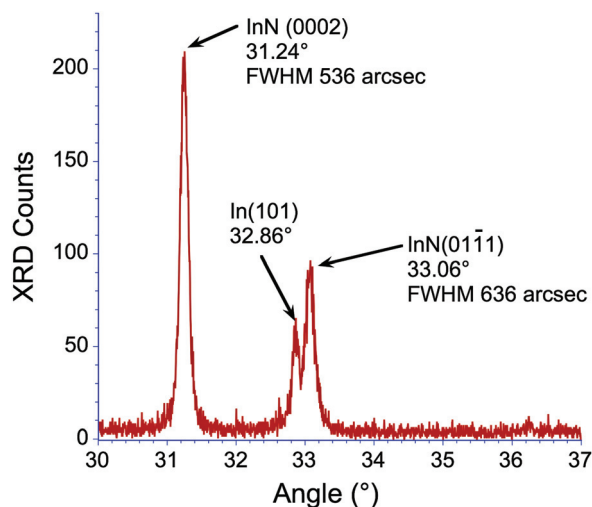


FIG. 2. (Color online) X-ray diffraction results of HPCVD-grown InN in ω - 2θ geometry.

The indium on the surface can be removed by 2 min wet etching in HCl after which the In (101) Bragg reflex at 32.86° is not observed anymore. The second peak located at 33.06° (2.707 \AA) with an FWHM of 636 arcsec is attributed to tilted crystallites exposing InN (01 $\bar{1}$ 1) facets.³²

Previous HREELS studies by the authors on InN epilayers grown on GaN/sapphire templates^{33–35} showed a strong loss feature at 550 cm^{-1} , which has been assigned to a Fuchs–Kliewer surface phonon. The loss peak at 3260 cm^{-1} for the atomic hydrogen cleaned surface was assigned to an N–H stretching vibration, while the loss feature at 870 cm^{-1} was assigned to an N–H bending vibration. From these observations it was concluded that the InN film in that previous work was N-polar and N–H terminated. In one study, a broad loss feature was assigned to a conduction band plasmon excitation and spectra acquired as a function of incident energy revealed the presence of a surface electron accumulation.³⁴

In the present work, a high resolution electron energy loss (HREEL) spectrum was acquired from the InN sample after atomic-hydrogen cleaning and is shown in Fig. 3. Vibrational loss features are observed at 640, 1260, 1440, 1600, 2960, 3400, and 3710 cm^{-1} . However, no loss features related to a conduction band plasmon are observed at loss energies up to 4500 cm^{-1} , indicating the layer has a relatively high carrier concentration.

The loss peaks at 1260, 1600 and 3400 cm^{-1} indicate that the dominant surface species is NH₂ as opposed to the NH observed in the earlier work.^{33–35} The loss feature at 3400 cm^{-1} is assigned to an NH₂ stretching vibration in agreement with that assigned by Tanaka *et al.*³⁶ for NH₂ symmetric stretching vibration on InP (110). The loss features at 1260 and at 1600 cm^{-1} are assigned to NH₂ wagging and scissor modes of vibration which have close agreement with those assigned by Tindall and Hemminger³⁷ on Ge (100). Bhatta *et al.*³⁵ reported a strong but sharp loss feature at 550 cm^{-1} on InN(000 $\bar{1}$) which they assigned to Fuchs–Kliewer surface phonon and Tindall and Hemminger³⁷ reported a

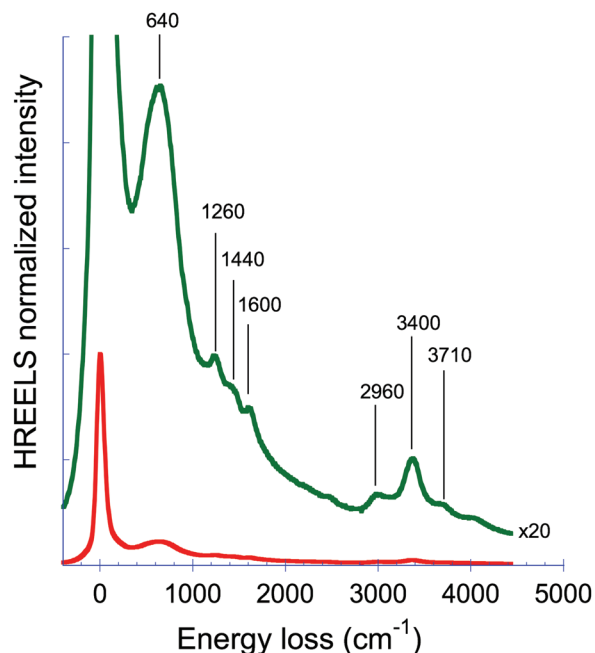


FIG. 3. (Color online) HREEL spectra of HPCVD-grown InN after atomic hydrogen cleaning.

rocking mode of NH₂ vibration at 884 cm^{-1} . Instead of these two individual loss features, a strong and broad loss feature has been observed at 640 cm^{-1} in this work. This strong and broad loss feature is assigned to the unresolved overlap of the Fuchs–Kliewer surface phonon and the rocking mode of the NH₂ vibration. A small C–H stretch vibrational peak is observed at 2960 cm^{-1} due to residual carbon. Though no carbon was seen in AES after a few cycles of sputtering followed by atomic hydrogen cleaning, the HREEL spectrum shows a little carbon contaminant on the surface since HREELS is more sensitive than AES. Small loss features at 1440 and at 3710 cm^{-1} have been assigned to the bending mode of C–H and the stretching mode of O–H, respectively. Nienhaus *et al.*³⁸ reported the InH stretching vibration at 1650 – 1700 cm^{-1} in HREELS experiments and at 1630 – 1650 cm^{-1} from *ab initio* calculations³⁹ on InP surfaces. However, no loss feature in this range was observed in the present work, indicating no surface InH exists on the atomic hydrogen cleaned surface. HREELS spectra (not shown) were also taken from the sample dosed with hydrogen at temperature as low as 60°C . But no loss feature related to InH was observed in the HREEL spectra. Although surface metallic indium was indicated in XRD, the sample was sputtered to remove contaminants before taking the HREELS measurements which showed no indium-related vibrations on the surface. The various loss features and their assignments have been summarized in Table II.

The Raman spectroscopic analysis indicates the existence of non-*c*-plane crystallites at or near the InN surface. The existence of such non-*c*-plane crystallites is further supported by XRD results, which show the presence of tilted (01 $\bar{1}$ 1) InN facets.³² Similarly, the observation of NH₂ rather than NH surface species indicates a non-*c*-plane surface orientation. In the wurtzite structure (01 $\bar{1}$ 1) facets are semipolar

TABLE II. HREELS vibrational frequencies and assignments for atomic hydrogen cleaned InN.

Frequency (cm ⁻¹)	Assignment
640	Fuchs-Kliewer phonon + NH ₂ rock
1260	NH ₂ wag
1440	C-H bend
1600	NH ₂ scissor
2960	C-H stretch
3400	NH ₂ stretch
3710	O-H stretch

and both In and N atoms would be expected to be present at the surface. However, in the HREEL spectrum no loss features attributable to InH are observed but only NH₂ vibrations. It is suggested that surface indium atoms are either not present or not available for reaction with atomic hydrogen. No surface reconstruction was observed in low energy electron diffraction due to the polycrystalline nature of the layer. If indium atoms were present and reactive, exposure to atomic hydrogen near room temperature should have produced InH vibrations in HREELS. From the HREELS spectrum, it can be concluded that the presence of NH₂ species on InN layer is due to the tilted facets, consistent with the XRD and Raman spectroscopy results.

It is expected that the presence of tilted planes may change the piezoelectric polarization properties of the surface¹⁷ as well as any surface electron accumulation.^{40,41} Both of these effects may impact the properties of heterojunction interfaces or metallic contacts. The predominance of NH₂ species on the surface, in contrast to the NH termination observed on *c*-plane oriented layers, indicates that these tilted planes may also exhibit differences in surface chemistry that can affect growth and processing.

The growth of tilted planes and the appearance of NH₂ related vibrational modes on the surface may be due to the growth of microcrystals associated with a 3D crystal growth mode. Two possible reasons reported for the 3D growth of InN are insufficient adatom surface diffusion due to nitrogen-rich growth conditions, i.e., high V/III ratio condition, and strain produced by lattice mismatch between InN and the substrate.⁴² In previous studies of HPCVD-grown InN layers by the authors,^{33–35} *c*-plane orientation was observed from layers grown on GaN buffer layers on the sapphire substrate (lattice mismatch between GaN and InN ~10%). In the present work, growth occurred directly on sapphire with no buffer layer (lattice mismatch between InN and sapphire ~29%). The strain due to the larger lattice mismatch may be a cause for the growth of tilted crystallites. However, the V–III precursor ratio may also be a contributing factor. The *c*-plane oriented layers in the author's previous work were grown with lower ammonia to TMI ratios (as low as 630) than the layer exhibiting tilted planes studied in the present work (ammonia to TMI ratio of 3000). Other parameters, such as, pressure, temperature, and precursor flow rate were similar between the present work and the previous studies. When V/III ratio is high, there is insufficient adatom surface diffusion due to nitrogen-rich growth conditions. Lattice

mismatch may lead to the formation of 3D islands during epitaxy to relieve the film strain.⁴² The present work suggests that sapphire substrate and high NH₃ to TMI ratio are key factors for the growth of InN layers in different orientations other than *c* plane.

The present work shows correlations between characterizations of surface and bulk structure and bonding on InN (01 $\bar{1}$ 1) facets but additional work is needed to investigate the effects on interface and device properties. Since the performance of InN-based devices depends upon the surface orientation, the study of chemical reactivity and thermal stability on the tilted planes may be of importance. In the authors' research group the study of surface reactions and thermal stability on the tilted InN planes is in progress.

IV. CONCLUSION

In summary, the structural properties of an InN layer grown on sapphire were studied by Raman spectroscopy, XRD, and HREELS. The Raman analysis shows the appearance of both mode pairs, A₁(LO)–E₂(high) and A₁(TO)–E₁(TO), due to the presence of tilted InN facets in the layer. XRD shows an additional Bragg reflex at 33.06° supporting the presence of tilted (01 $\bar{1}$ 1) InN crystallites. The tilted orientation of the crystals results in an InN surface mainly consisting of NH₂ species as observed in HREELS in contrast to the NH vibrations observed from the InN (0001) surface. Growth of tilted planes in InN is a consequence of a 3D growth mode suggested to be due to the high V/III ratio and large lattice mismatch with the sapphire substrate.

¹R. Juza and H. Hahn, *Z. Anorg. Allg. Chem.* **239**, 282 (1938).

²H. Lu, W. J. Schaff, and L. F. Eastman, *J. Appl. Phys.* **96**, 3577 (2004).

³M. Singh and J. Singh, *J. Appl. Phys.* **94**, 2498 (2003).

⁴A. Yamamoto, Md. R. Islam, T. Kang, and A. Hashimoto, *Phys. Status Solidi C* **7**, 1309 (2010).

⁵S. Yamaguchi, R. Izaki, N. Kaiwa, S. Sugimura, and A. Yamamoto, *Appl. Phys. Lett.* **84**, 5344 (2004).

⁶Y. M. Meziani, B. Maleyre, M. L. Sadowski, S. Ruffenach, O. Briot, and W. Knap, *Phys. Status Solidi A* **202**, 590 (2005).

⁷I. Akasaki, H. Amano, N. Koide, M. Kotaki, and K. Manabe, *Physica B* **185**, 428 (1993).

⁸S. Nakamura, M. Senoh, and T. Mukai, *Jpn. J. Appl. Phys., Part 2* **32**, L8 (1993).

⁹S. Nakamura, M. Senoh, S. Nagahama, N. Iwasa, T. Yamada, T. Matsushita, H. Kiyoku, and Y. Sugimoto, *Jpn. J. Appl. Phys., Part 2* **35**, L74 (1996).

¹⁰M. Buegler, M. Alevli, R. Atalay, G. Durkaya, I. Senevirathna, M. Jamil, I. Ferguson, and N. Dietz, *Proc. SPIE* **7422**, 742218 (2009).

¹¹S. N. Mohammad and H. Morkoc, *Prog. Quantum Electron.* **20**, 361 (1996).

¹²A. G. Bhuiyan, A. Hashimoto, and A. Yamamoto, *J. Appl. Phys.* **94**, 2779 (2003).

¹³N. Dietz, M. Strassburg, and V. Woods, *J. Vac. Sci. Technol. A* **23**, 1221 (2005).

¹⁴J. MacChesney, P. M. Bridenbaugh, and P. B. O'Connor, *Mater. Res. Bull.* **5**, 783 (1970).

¹⁵N. Dietz, in *III-Nitrides Semiconductor Materials*, edited by Z. C. Feng (Imperial College Press, London, 2006), p.203.

¹⁶S. Schwaiger, F. Lipski, T. Wunderer, and F. Scholz, *Phys. Status Solidi C* **7**, 2069 (2010).

¹⁷P. Lefebvre, A. Morel, M. Gallard, T. Talierco, J. Allegre, B. Gil, H. Mathieu, B. Damilano, N. Grandjean, and J. Massies, *Appl. Phys. Lett.* **78**, 1252 (2001).

- ¹⁸P. Waltereit, O. Brandt, A. Trampert, H. T. Grahn, J. Menniger, M. Ramsteiner, M. Reiche, and K. H. Ploog, *Nature (London)* **406**, 865 (2000).
- ¹⁹K. Kusakabe, S. Ando, and K. Ohkawa, *J. Cryst. Growth* **298**, 293 (2007).
- ²⁰H. Ahn, Y. P. Ku, C. H. Chuang, C. L. Pan, H. W. Lin, Y. L. Hong, and S. Gwo, *Appl. Phys. Lett.* **92**, 102103 (2008).
- ²¹H. Naoi, D. Muto, T. Hioka, Y. Hayakawa, A. Sujuki, T. Araki, and Y. Nanishi, *Phys. Status Solidi B* **244**, 1834 (2007).
- ²²R. P. Bhatta, B. D. Thoms, M. Alevli, and N. Dietz, *Surf. Sci.* **602**, 1428 (2008).
- ²³N. Dietz, M. Alevli, V. Woods, M. Strassburg, H. Kang, and I. T. Ferguson, *Phys. Status Solidi B* **242**, 2985 (2005).
- ²⁴V. Woods and N. Dietz, *Mater. Sci. Eng., B* **B127**, 239 (2006).
- ²⁵V. J. Bellitto, B. D. Thoms, D. D. Koleske, A. E. Wickenden, and R. L. Henry, *Surf. Sci.* **430**, 80 (1999).
- ²⁶L. F. J. Piper, T. D. Veal, M. Walker, I. Mahboob, C. F. McConville, H. Lu, and W. J. Schaff, *J. Vac. Sci. Technol. A* **23**, 617 (2005).
- ²⁷A. Kasic, M. Schubert, Y. Saito, Y. Nanishi, and G. Wanger, *Phys. Rev. B* **65**, 115206 (2002).
- ²⁸T. Inushima, T. Shiraiishi, and V. Yu. Davydov, *Solid State Commun.* **110**, 491 (1999).
- ²⁹J. S. Dyck, K. Kim, S. Limpijumnong, W. R. L. Lambrecht, K. Kash, and J. C. Angus, *Solid State Commun.* **114**, 355 (2000).
- ³⁰S. Dhara *et al.*, *Appl. Phys. Lett.* **88**, 241904 (2006).
- ³¹T. V. Shubina *et al.*, *Phys. Rev. Lett.* **92**, 117407 (2004).
- ³²K. M. Yu *et al.*, *Appl. Phys. Lett.* **86**, 071910 (2005).
- ³³R. P. Bhatta, B. D. Thoms, M. Alevli, V. Woods, and N. Dietz, *Appl. Phys. Lett.* **88**, 122112 (2006).
- ³⁴R. P. Bhatta, B. D. Thoms, M. Alevli, and N. Dietz, *Surf. Sci.* **601**, L120 (2007).
- ³⁵R. P. Bhatta, B. D. Thoms, A. Weerasekera, A. G. U. Perera, M. Alevli, and N. Dietz, *J. Vac. Sci. Technol. A* **25**, 967 (2007).
- ³⁶S. Tanaka, M. Onchi, and M. Nishijima, *Surf. Sci.* **191**, L756 (1987).
- ³⁷C. Tindall and J. C. Hemminger, *Surf. Sci.* **330**, 67 (1995).
- ³⁸H. Nienhaus, S. P. Grabowski, and W. Monch, *Surf. Sci.* **368**, 196 (1996).
- ³⁹J. Fritsch, A. Echert, P. Pavone, and U. Schroder, *J. Phys. Condens. Matter* **7**, 7717 (1995).
- ⁴⁰C. G. Van de Walle and D. Segev, *J. Appl. Phys.* **101**, 081704 (2007).
- ⁴¹V. Darakchieva *et al.*, *Appl. Phys. Lett.* **95**, 202103 (2009).
- ⁴²B. Liu, T. Kitajima, D. Chen, and S. R. Leone, *J. Vac. Sci. Technol. A* **23**, 304 (2005).